www.czasopisma.pan.pl PAN www.journals.pan.pl

ARCHIVES of FOUNDRY ENGINEERING

ISSN (2299-2944)
Volume 18
Issue 4/2018

65 – 70

13/4

DOI: 10.24425/afe.2018.125170

Published quarterly as the organ of the Foundry Commission of the Polish Academy of Sciences

Microstructure and Fatigue Life of the Binary Lead-free Alloys with High Zn Content

K. Pietrzak [a, *], A. Klasik [b], M. Maj [c, **], N. Sobczak [a, d]

[a] Institute of Precision Mechanics, 3 Duchnicka Str. 01-796 Warsaw, Poland
[b] Motor Transport Institute, 80 Jagiellońska Str. 03-301 Warsaw, Poland
[c] AGH University of Science and Technology, Faculty of Foundry Engineering, 23 Reymonta Str. 30-059 Cracow, Poland
[d] Foundry Research Institute, 73 Zakopiańska Str. 30-418 Cracow, Poland
Corresponding authors. E-mail address: * krystyna.pietrzak@imp.edu.pl, ** mmaj@agh.edu.pl

Received 17.05.2018; accepted in revised form 05.10.2018

Abstract

The results of studies presented in this article are an example of the research activity of the authors related to lead-free alloys. The studies covered binary SnZn90 and SnZn95 lead-free alloys, including their microstructure and complex mechanical characteristics.
The microstructure was examined by both light microscopy (LM) and scanning electron microscopy (SEM). The identification of alloy chemical composition in micro-areas was performed by SEM/EDS method. As regards light microscopy, the assessment was of both qualitative and quantitative character. The determination of the geometrical parameters of microstructure was based on an original combinatorial method using phase quantum theory.
Comprehensive characterization of mechanical behavior with a focus on fatigue life of alloys was performed by means of the original modified low cycle fatigue method (MLCF) adapted to the actually available test machine. The article discusses the fatigue life of binary SnZn90 and SnZn95 alloys in terms of their microstructure. Additionally, the benefits resulting from the use of the combinatorial method in microstructure examinations and MLCF test in the quick estimation of several mechanical parameters have been underlined.

Keywords: Lead-free alloy, Microstructure, Mechanical properties

1. Introduction

When searching for literature data on lead-free alloys, many research papers containing results of the development of new chemical compositions of alloys can be encountered.

Lead-free alloys take a special position in soldering processes because of the EU Directives prohibiting the use of lead in industrial practice.

Lead-free solder alloys are still extensively studied in terms of their use in soldering processes, including high-temperature applications.

The issues of lead-free solders and the possibilities of their application in practice were the inspiration for two European initiatives COST ACTION531 [1] and COST ACTION 0602 [2], in which the authors of this research also took part.

The outcome was a number of useful material data, including both lead-free alloys and soldered joints with various substrates. The data included microstructure, wettability, mechanical

properties determined in a static tensile test, corrosion resistance, shear strength, resistance to thermal shocks, etc. [1,2].

The binary SnZn9 alloy is very popular due to its melting temperature of 198 °C, comparable to the melting temperature of Sn-Pb alloys equal to 183 °C, satisfactory mechanical properties and low cost.

Unfortunately, they are characterized by unsatisfactory wettability because Zn is easily oxidized, which is the reason for the formation of an oxidized layer. This demands the use of special fluxes and other means of protection in the manufacture of soldered joints [3]. The improvement of properties can also be achieved by introducing trace amounts of other elements, e.g. Bi, into the alloy.

The authors of [4-9], investigating Zn-xSn alloys in which the Sn content in the alloy is 20%, 30% and 40% have concluded that these alloys may be considered a new class of lead-free solders intended for high temperature applications.

Their usefulness results from a number of favorable properties such as high melting point, high strength, high ductility compared to other Zn-based alloys, very good electrical properties, resistance to oxidation at high temperature and in a humid environment, and – last but not least - low price.

Kudyba et al [10] reported that an increase in the test temperature by 50°C above the melting point of a solder significantly improves its solderability of Ni since the nickel substrate becomes fully wettable ($\theta = 0$ °) while that the maximum wetting force Fmax raises quite considerably up to a value above 6 mN.

Despite the fact that current research is conducted in a systematic way, when searching for literature data, it is impossible to find, for example, information on the fatigue properties of alloys being developed, and in particular on the mechanical parameters, including fatigue parameters, evaluated from the measurement data collected on a single sample only.

Therefore, since some time, the authors of this article have undertaken and continue to undertake this type of research, publishing systematically the results obtained.

The results presented now are an example of this type of activity.

2. Materials

Lead-free binary alloys with high Zn content were subjected to material testing, including both microstructure and complex mechanical characteristics, as well as fatigue behavior.

Test alloys were made by the Foundry Research Institute in Cracow and supplied in the form of ready-to-use cast samples for mechanical testing. Metals characterized by the purity of 99.9% were used for the preparation of both SnZn90 and SnZn95 alloys.

The metals were melted in a graphite crucible under argon atmosphere and then they were cast into a graphite mold that allowed obtaining ready-to-use samples. The dimensions of specimens were as follow: total length 140 mm and measuring diameter 8 mm.

The casting process was carried out at a temperature of about 50 °C above the liquidus line.

The samples were used for both mechanical testing and microstructure examinations. The metallographic assessment was carried out on the cross-sections prepared from the grip section of samples.

According to this procedure, different measurement data are always collected on the same sample, which reduces to minimum the effect of possible microstructural heterogeneities.

Before further research was undertaken, castings had been subjected to chemical control analysis. The analyzes of the chemical composition were performed by X-ray microfluorescence method using the Niton XL3t XRF analyzer.

The aim of the analysis was to determine whether the composition of both alloys is repeatable. The results are summarized in Table 1.

Table 1.
Content of the basic components in SnZn90 and SnZn95 alloys

Sample No.	SnZn90 alloy		SnZn95 alloy	
	Sn [wt. %]	Zn [wt. %]	Sn [wt. %]	Zn [wt. %]
1	9.2	90.7	4.8	95.0
2	9.1	90.8	4.8	95.1
3	9.3	90.5	4.6	95.3
4	8.9	91.0	4.7	95.3
5	9.1	90.8	4.7	95.2
6	9.0	90.9	4.5	95.4

The values compiled in Table 1 indicate that stable chemical composition was obtained in both SnZn90 and SnZn95 alloys.

3. Microstructure

In order to determine the effect of the microstructure of both alloys on their mechanical characteristics, microstructure examinations using light microscopy (LM – Olympus PMG3 coupled on line with CLEMEX image analyzer) and SEM (JEOL 6306 LA) method were carried out. Microstructures of both alloys are shown in Figures 1 and 2. The presented photographs illustrate only the type of microstructure that is characteristic for both alloys and consists of (αZn+βSn) eutectic precipitates distributed in the αZn solid solution.

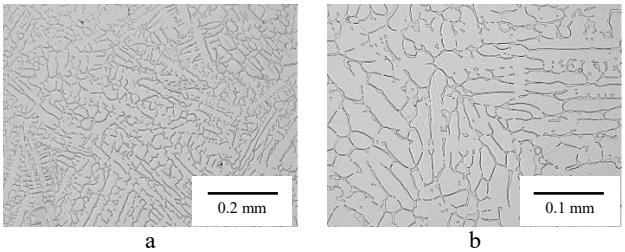

a b

Fig. 1. Microstructure of SnZn90 alloy: a) magn. 100x, b) magn. 200x

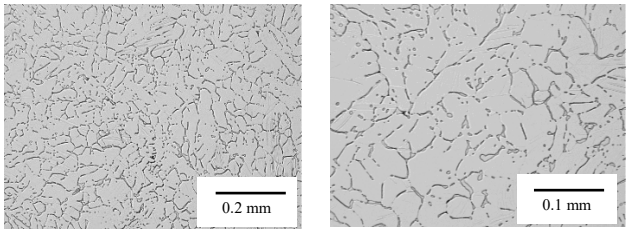

a b

Fig 2. Microstructure of SnZn95 alloy: a) magn. 100x, b) magn. 200x

Figure 3 shows an example of microstructure identification obtained by SEM/EDS method. Figure 3a relates to the primary grains of αZn solid solution in SnZn90 alloy and Figure 3b to the (αZn+βSn) eutectic precipitates in that alloy. Due to the fact that both SnZn90 and SnZn95 alloys are characterized by the same type of microstructure, the results of chemical analysis in micro-areas (made also for the alloy with higher Zn content of 95%) are not presented in this article.

On the other hand, based on the observations made by light microscopy, it was found that microstructures of both examined alloys differed in the content of eutectic precipitates. This effect results from the Zn content in the alloys.

It was assumed that the difference in the content of eutectic precipitates as well as their size and distribution in the matrix can significantly affect the mechanical characteristics of both alloys.

Therefore, further metallographic examinations were carried out by quantitative metallographic methods. To determine the geometrical parameters of eutectic precipitates, a combinatorial method resulting from the phase quantum theory was used. Its essence consists in the determination of two estimators only, i.e. the estimator of the volume fraction (V_V) and the estimator of the relative surface (N_L) of the microstructural elements which are the target of research. Both estimators are the basis for further determination of the required geometrical parameters using the developed calculation formulas [11]. It should also be emphasized that this method has been many times positively verified by the authors.

Quantitative research was carried out at a microscopic magnification of 200x in 100 measurement fields of the sample. The area of a unit measurement field was 0.075 mm^2. The total measurement area in the sample was 7.5 mm^2. Based on the results of quantitative measurements and calculations of eutectic precipitates, the following geometrical parameters were determined: volume fraction (V_V), estimator of relative area (N_L), mean chord (l_{avg}) and the mean free distance between precipitates (λ).

The results of the measurements and calculations are presented in Table 2 for the SnZn90 alloy and in Table 3 for the SnZn95 alloy.

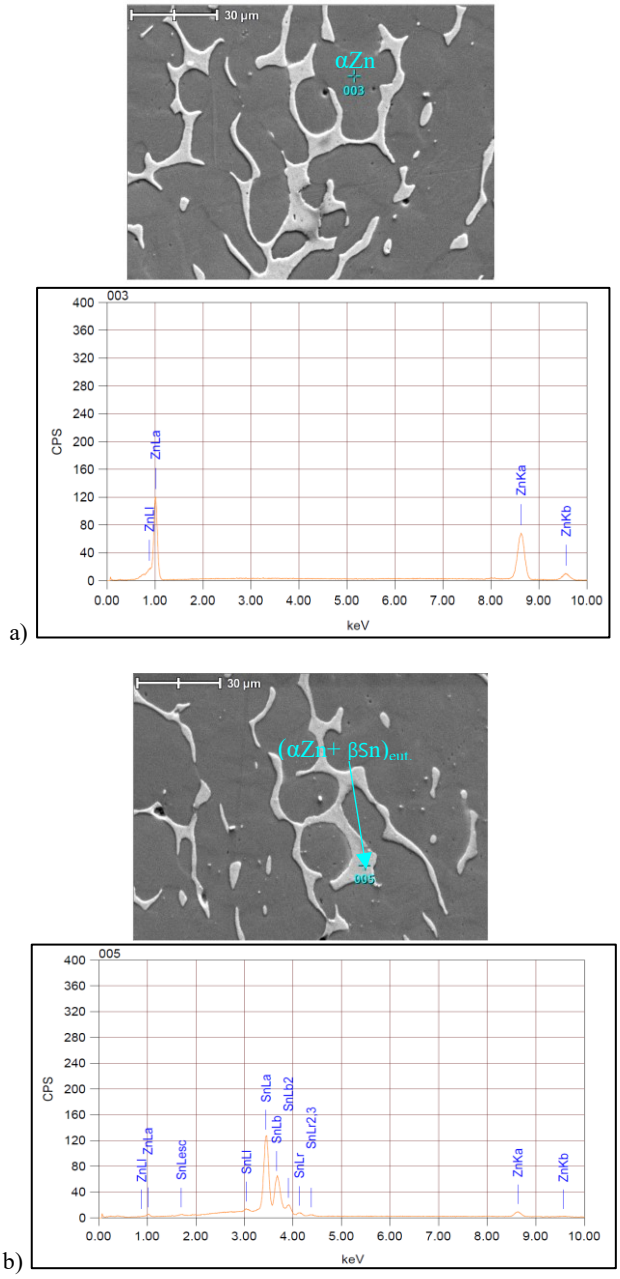

Fig. 3. Example of SEM/EDS results obtained for SnZn90 alloy: a) in the area of primary grains of αZn solid solution, b) in the area of (αZn+βSn) eutectic precipitates

The results summarized in these tables indicate that for both SnZn90 and SnZn95 alloys, the differences in the values of all the parameters determined for individual samples are small as evidenced by the values of standard deviation given in Tables 2 and 3.

The observed differences are also presented in the form of diagrams in Figures 4-7.

Table 2.
Selected geometrical parameters of (α-Zn+β-Sn) eutectic precipitates in the examined binary SnZn90 alloy

Sample No.	V_{Vavg} [%]	N_{Lavg} [1/mm]	l_{avg} [μm]	λ_{avg} [μm]
1	19.0	37.3	5	27
2	19.1	36.8	4	26
3	19.2	36.9	4	29
4	19.3	38.1	5	25
5	18.6	37.4	6	26
6	18.9	37.1	6	28
Mean value	19.0	37.2	5	27
St. Dev.	0.2	0.5	1	2

Table 3.
Selected geometrical parameters of (α-Zn+β-Sn) eutectic precipitates in the examined SnZn95 alloy

Sample No.	V_{Vavg} [%]	N_{Lavg} [1/mm]	l_{avg} [μm]	λ_{avg} [μm]
1	11.5	24.1	5	37
2	12.1	26.0	6	37
3	10.9	23.8	4	39
4	11.2	24.3	6	37
5	12.3	23.2	5	36
6	10.8	24.0	4	38
Mean value	11.4	24.2	5	37
St. Dev.	0.6	0.9	1	1

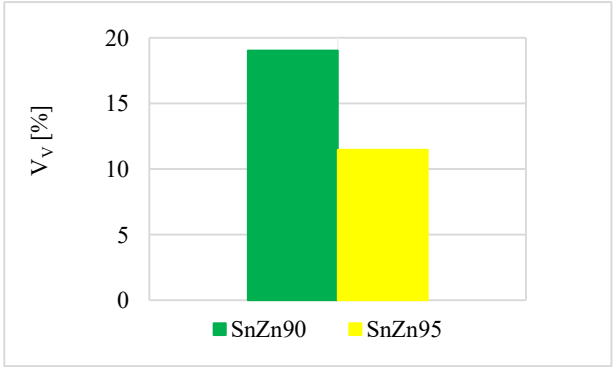

Fig. 4. Volume fraction of (α-Zn+β-Sn) eutectic precipitates in the examined binary alloys with high Zn content

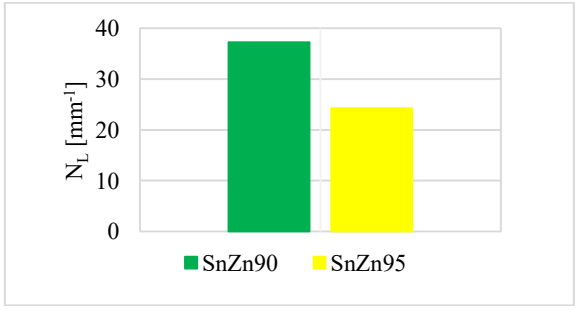

Fig. 5. Estimator of relative area (N_L) of (α-Zn+β-Sn) eutectic precipitates in the examined binary alloys with high Zn content

In contrast, the dimensions of eutectic precipitates are the same for both examined alloys (Fig. 6).

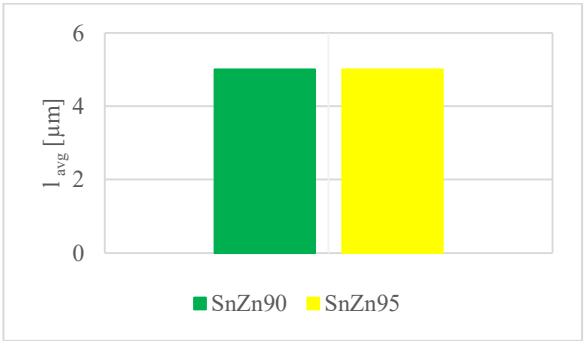

Fig. 6. Mean chord (l_{avg}) of (α-Zn+β-Sn) eutectic precipitates in the examined binary alloys with high Zn content

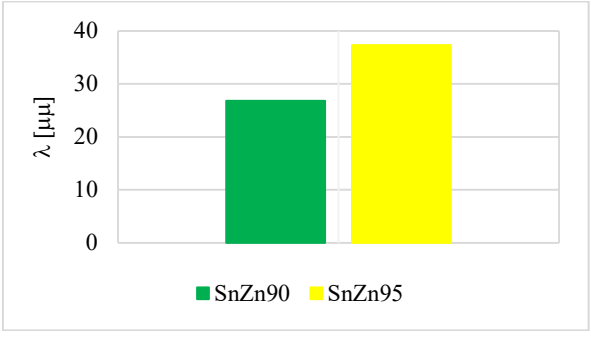

Fig. 7. Mean free distance (λ) between (α-Zn+β-Sn) eutectic precipitates in the examined binary alloys with high Zn content

The analysis of the comparative graphs presented in Figures 4-7 leads to the conclusion that the volume fraction (V_V) of eutectic precipitates and the estimator of their relative surface area (N_L) are higher in the SnZn90 alloy (Figs. 4 and 5, respectively). Thus, the same chord (l) of the precipitates and higher volume fraction (V_V) and estimator of the relative area (N_L) are directly responsible for the smaller free distance (λ) between these precipitates.

This effect was observed in the SnZn90 alloy (Fig. 7).

4. Mechanical properties

To obtain comprehensive mechanical characteristics of the SnZn90 and SnZn95 alloys in as cast state, a modified low cycle fatigue test (MLCF) was carried out. The theoretical and methodological fundamentals of this method are described, for example, in [12, 13]. The authors of this article want to emphasize once again the fact that the presented measurement procedure allows quick estimation of over a dozen mechanical parameters based on measurement data coming from one sample. This practically eliminates the influence of microstructural heterogeneities, which is particularly important in the studies of cast materials. Based on the MLCF method and using INSTRON 8874 testing machine, the following mechanical parameters were

determined: R_m (ultimate tensile strength), $R_{0.02}$ (apparent elastic limit), $R_{0.2}$ (yield point), Z_{go} (fatigue limit assessed from the developed experimental curve [12, 13] considered the key element of the MLCF method), K' (cyclic strength coefficient), R_a (accommodation limit defined as a limit stress above which the stabilization of permanent deformation occurs no longer [12]), Young's modulus, b – Basquin's coefficient (fatigue strength exponent), c - fatigue ductility exponent, ε_{max} - maximum allowable permanent strain, n' – cyclic strain hardening exponent. The course of deformation was recorded during unilateral cycling of SnZn90 and SnZn95 alloys. The MLCF tests were stress-controlled. During test, the stress was increased in subsequent groups of measurement cycles. An example of the stress-strain diagram is shown in Figure 7.

As follows from the graphs, a significantly higher deformability was noticed in the SnZn90 alloy (Fig. 7a) and it was obtained at a stress higher than in the SnZn95 alloy (Fig. 7b).

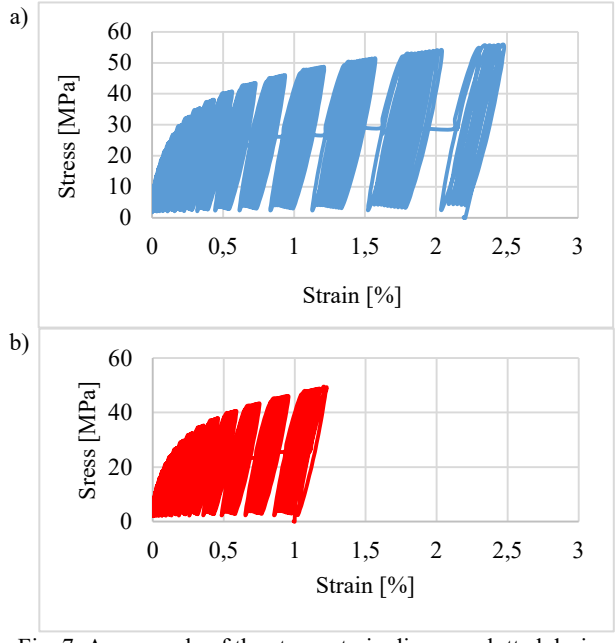

Fig. 7. An example of the stress-strain diagram plotted during unilateral cycling of SnZn90 (a) and SnZn95 (b) alloys

The mean values of mechanical parameters determined by the MLCF method are presented in Figures 8-10.

The mechanical parameters such as R_m, $R_{0.02}$, $R_{0.2}$, Z_{go}, K' and R_a determined for both examined alloys are shown in Figure 8, while Young's modulus is shown in Figure 9.

From the values of the mechanical parameters shown in Figures 8 and 9 it follows that most of them are higher in the SnZn90 alloy. This is due to the microstructure of this alloy containing (α-Zn + β-Sn) eutectic precipitates uniformly distributed in the alloy matrix.

Moreover, in the case of the SnZn90 alloy, the volume fraction of these precipitates is larger and the mean free distance between them is smaller compared to SnZn95 alloy. This fact has a positive effect on the mechanical parameters shown in respective graphs (Figs. 8 and 9).

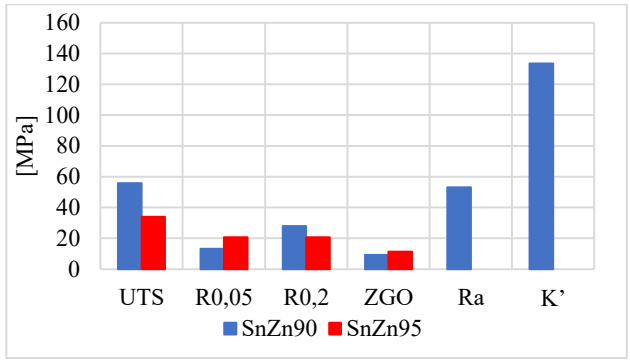

Fig. 8. Mechanical parameters of the examined binary alloys: R_m $R_{0.02}$, $R_{0.2}$, Z_{go}, K' and R_a

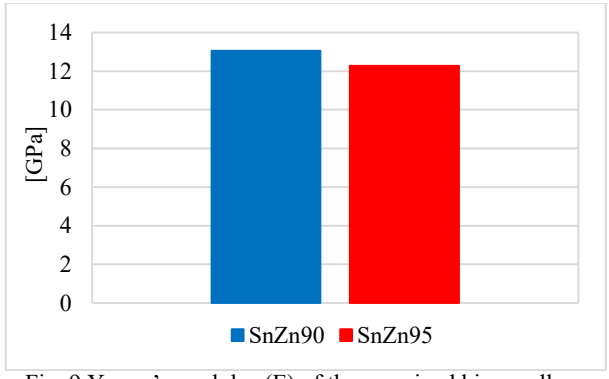

Fig. 9 Young's modulus (E) of the examined binary alloys

In contrast, Figure 10 shows the values of selected fatigue parameters such as b - Basquin's coefficient (fatigue strength exponent), c - fatigue ductility exponent, ε_{max} - maximum allowable permanent strain; n′ - cyclic strain hardening exponent.

The values of fatigue parameters *b* and *c* should be comprised within specified limits. For parameter *b* it is the range from -0.05 to - 0.15 and for parameter *c* it is the range from -0.5 to -0.7 [14]. From the values presented in Figure 10 it follows that these conditions are met.

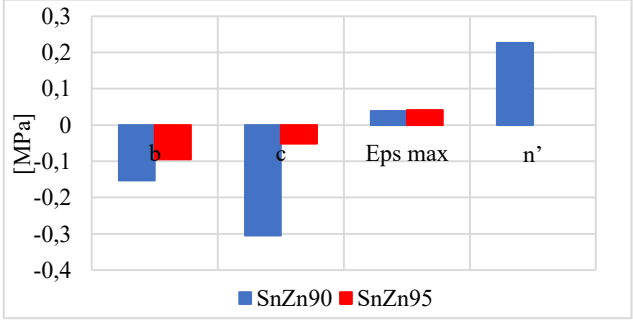

Fig. 10. Selected fatigue parameters of the examined binary alloys: b- Basquin's coefficient (fatigue strength exponent), c- fatigue ductility exponent, ε_{max} -maximum allowable permanent strain; n′- cyclic strain hardening exponent

At the same time it is easy to notice that, compared to SnZn95 alloy, the fatigue strength exponent (b) assumes a lower value in

the SnZn90 alloy (its absolute value is higher), which means that the fatigue strength of the SnZn90 alloy is inferior to the fatigue strength of SnZn95 alloy (Figs. 8 and 10). The fatigue ductility exponent (c) is also lower in the SnZn90 alloy (its absolute value is higher) when compared to SnZn95 alloy, which means that the SnZn90 alloy is characterized by higher ductility (Figs. 7a and 10). Summing up, it can be concluded that, due to more favorable microstructural parameters, the SnZn90 alloy is characterized by higher values of the majority of the determined mechanical parameters. Only parameters related to fatigue strength (b) and Z_{go} are lower in this alloy. It shows how small changes in microstructure morphology can affect fatigue properties.

Therefore, depending on the intended applications, it is advisable to determine the most complex mechanical characteristics as allowed by the MLCF method and to quantify the microstructure, which in turn enables determining which microstructural factors play a fundamental role in the mechanical behavior of materials.

5. Conclusions

Based on the results obtained it is possible to formulate the following conclusions.

- The examined SnZn90 and SnZn95 alloys are both characterized by stable chemical composition.
- The microstructural differences observed in the two examined alloys are mainly related to the volume fraction (V_V) of eutectic precipitates and mean free distance between them, both of which significantly affect the mechanical behavior of alloys.
- The majority of the determined mechanical parameters assume higher values in the SnZn90 alloy, mainly due to a higher volume fraction (V_V) of the eutectic precipitates uniformly distributed in metal matrix and smaller mean free distance (λ) between them.
- Only two fatigue parameters, i.e. the fatigue strength exponent (b) and Z_{go}, assume lower values in the SnZn90 alloy. It means that higher volume fraction (V_V) of eutectic precipitates and smaller mean free distance (λ) between them exert an adverse effect on material subjected to cyclic loading. In this case, the cause is the large number of microstructural notches.

Acknowledgments

The article was in part based on research carried out within the framework of the EU COST ACTION MP0602 with financial support from the Ministry of Science and Higher Education of Poland.

References

[1] Schmetterer, C., Ipser, H., Pearce, J. (2008). *Lead-Free Solders: Handbook of Properties of SAC Solders and Joints*. ELFNET COST 531+Lead-Free solders vol. 2, ISBN: 978-80-86292-27-4.
[2] Kroupa, A. (2012). *Handbook of High-Temperature Lead-Free Solders*. Volume 3: Group Project Reports. COST MP0602, ISBN: 978-80-905363-3-3.
[3] Kotadia, H.R., Howes, P.D. & Mannan, S.H. (2014). A review: On the development of low melting temperature Pb-free solders. *Microelectronics Reliability*. 54, 1253-1273.
[4] Zeng, G., McDonald, S., Nogita, K. (2012). Development of high-temperature solders: Review. *Microelectronics Reliability*. 52, 1306-1322.
[5] Lee, J-E., Kim, K-S., Suganuma, K., Inoue, M. & Izuta, G. (2007). Thermal Properties and Phase Stability of Zn-Sn and Zn-In Alloys as High Temperature Lead-Free Solder. *Materials Transactions*. 48, 3, 584-593.
[6] Mahmudi, R. & Eslami, M. (2011). Shear strength of the Zn–Sn high-temperature lead-free solders. *J Mater Sci: Mater Electron*. 22, 1168-1172.
[7] Stamenkovic, U.S., Markovic, I., Dimitrijevic, M., Medic, D. (2017). SEM and EDS investigation of Zn-Sn alloys as potential high temperature lead-free solder. Proceedings of XXV International Conference "Ecological Truth" ECO-IST'17 (pp. 196-201).
[8] Park, S. (2013). High-power semiconductor die-attachment : Application of Zn with minor metal additions. Ph.D. Dissertation.
[9] Suganuma, K., Kim, S-J. & Kim, K.-S. (2009). High-Temperature Lead-Free Solders: Properties and Possibilities. *JOM*. 64-71.
[10] Kudyba, A., Siewiorek, A., Sobczak, N. (2012). Effect of zinc content and temperature on nickel solderability with Sn-xZn (x = 4.5, 90, 95 wt%) alloys. *Transactions of Foundry Research Institute*. LII, 4, 197-211.
[11] Kęsy, B.K. (1990). Microstructure as arrangement of unitary phase parts and stereological parameters Proceedings of 3rd Int. Conference on Stereology In Materials Science, Szczyrk, (pp. 226-231).
[12] Maj, M. (2012). *Fatigue life of selected foundry alloys.* Katowice-Gliwice: Wyd. Archives of Foundry Engineering. (in Polish).
[13] Maj, M., Klasik, A., Pietrzak, K. & Rudnik, D. (2015). Modified low-cycle fatigue (LCF) test *Metalurgija = Metallurgy.* 54(1), 207-210. ISSN 0543-5846.
[14] Kocańda, St., Kocańda, A. (1989). *Low-cycle fatigue strength of metals*. Warsaw: PWN.